1521-0103/365/3/614–623$35.00
THE JOURNAL OF PHARMACOLOGY AND EXPERIMENTAL THERAPEUTICS

https://doi.org/10.1124/jpet.118.247692
J Pharmacol Exp Ther 365:614–623, June 2018

New Targets for Old Drugs: Cardiac Glycosides Inhibit Atrial-Specific K_{2P}3.1 (TASK-1) Channels

Constanze Schmidt, Felix Wiedmann, Anne-Rike Gaubatz, Antonius Ratte, Hugo A. Katus, and Dierk Thomas

Department of Cardiology, Medical University Hospital Heidelberg, Heidelberg, Germany (C.S., F.W., A.-R.G., A.R., H.A.K., D.T.); Heidelberg Center for Heart Rhythm Disorders, University Hospital Heidelberg, Heidelberg, Germany (C.S., F.W., A.-R.G., A.R., H.A.K., D.T.); and German Centre for Cardiovascular Research, Heidelberg/Mannheim Partner Site, University of Heidelberg, Heidelberg, Germany (C.S., F.W., H.A.K., D.T.)

Received January 12, 2018; accepted April 4, 2018

ABSTRACT

Cardiac glycosides have been used in the treatment of arrhythmias for more than 200 years. Two-pore-domain (K_{2P}) potassium channels regulate cardiac action potential repolarization. Recently, K_{2P}3.1 [tandem of P domains in a weak inward rectifying K^+ channel (TWIK)–related acid-sensitive K^+ channel (TASK)-1] has been implicated in atrial fibrillation pathophysiology and was suggested as an atrial-selective antiarrhythmic drug target. We hypothesized that blockade of cardiac K_{2P} channels contributes to the mechanism of action of digitoxin and digoxin. All functional human K_{2P} channels were screened for interactions with cardiac glycosides. Human K_{2P} channel subunits were expressed in *Xenopus laevis* oocytes, and voltage clamp electrophysiology was used to record K^+ currents. Digitoxin significantly inhibited K_{2P}3.1 and K_{2P}16.1 channels. By contrast, digoxin displayed isolated inhibitory effects on K_{2P}3.1. K_{2P}3.1 outward currents were reduced by 80% (digitoxin, 1 Hz) and 78% (digoxin, 1 Hz). Digitoxin inhibited K_{2P}3.1 currents with an IC_{50} value of 7.4 μM. Outward rectification properties of the channel were not affected. Mutagenesis studies revealed that amino acid residues located at the cytoplasmic site of the K_{2P}3.1 channel pore form parts of a molecular binding site for cardiac glycosides. In conclusion, cardiac glycosides target human K_{2P} channels. The antiarrhythmic significance of repolarizing atrial K_{2P}3.1 current block by digoxin and digitoxin requires validation in translational and clinical studies.

Introduction

Effective and safe pharmacologic treatment of atrial fibrillation (AF) still constitutes an unmet need in cardiovascular medicine (Schmidt et al., 2011). Cardiac glycosides are widely used for rate control in AF in accordance with current guidelines (Kirchhof et al., 2016). Digoxin use has recently been associated with increased mortality in some retrospective analyses, whereas others indicated neutral effects of digoxin on survival (Ziff et al., 2015; Bavendiek et al., 2017). Despite the widespread use of digoxin and digitoxin, their effects on cardiovascular electrophysiology are insufficiently understood. We hypothesized that a more detailed understanding of the complex electrophysiological profile of cardiac glycosides is required to identify potential beneficial or adverse cellular mechanisms associated with their clinical use.

Two-pore-domain (K_{2P}) potassium channels facilitate action potential repolarization, and dynamic regulation of K_{2P} currents modulates cellular excitability (Goldstein et al., 2001). Multiple K_{2P} K^+ channel genes are expressed in human atrium (Schmidt et al., 2015). K_{2P}3.1 [or tandem of P domains in a weak inward rectifying K^+ channel (TWIK)–related acid-sensitive K^+ channel (TASK)-1] displays the highest atrial expression levels among functional K_{2P} channels, whereas ventricular K_{2P}3.1 abundance is negligible. Upregulation of K_{2P}3.1 contributes to atrial action potential shortening in patients with persistent or permanent AF (Schmidt et al., 2015). By contrast, action potential duration (APD) prolongation that is observed in atrial myocytes of patients with heart failure is related to downregulation of repolarizing K_{2P}3.1 channels (Schmidt et al., 2017). Inhibition by class III antiarrhythmic drugs or genetic inactivation of cardiac K_{2P} currents results in action potential prolongation, highlighting the physiologic significance of K_{2P} currents in atrial electrophysiology and a potential role as antiarrhythmic drug targets (Ravens, 2010; Donner et al., 2011; Schmidt et al., 2014, 2015; Hancox et al., 2016; Wiedmann et al., 2016; Chai et al., 2017).

This study was supported in part by research grants from the University of Heidelberg Faculty of Medicine [Rahel Goitein-Straus Scholarship and Olympia-Morata Scholarship (to C.S.)], the German Center for Cardiovascular Research [Excellence Grant (to C.S.)], the German Heart Foundation/German Foundation of Heart Research [Grants F/41/15 (to C.S.) and F/08/14 (to D.T.) and a Kaltenbach Scholarship (to A.R.)], Else Kröner-Fresenius-Stiftung [Grant 2014_A242 (to D.T.)], the Joachim Siebeneicher Foundation [(to D.T.)], the German Research Foundation [Grants SCHM 3358/1-1 (to C.S.) and TH 1120/7-1 (to D.T.)], the Ministry of Science, Research, and the Arts Baden-Wuerttemberg [Sonderlinie Medizin (to D.T.)]. F.W. was supported by a German Cardiac Society Otto-Hess Scholarship. D.T. reports receiving lecture fees/honoraria from Bayer Vital, Bristol-Myers Squibb, Daiichi Sankyo, Medtronic, Pfizer Pharma, Sanofi-Aventis, St. Jude Medical, and ZOLL CMS and research grant support from Daiichi Sankyo.
https://doi.org/10.1124/jpet.118.247692.

ABBREVIATIONS: AF, atrial fibrillation; APD, action potential duration; K_{2P}, two-pore-domain.

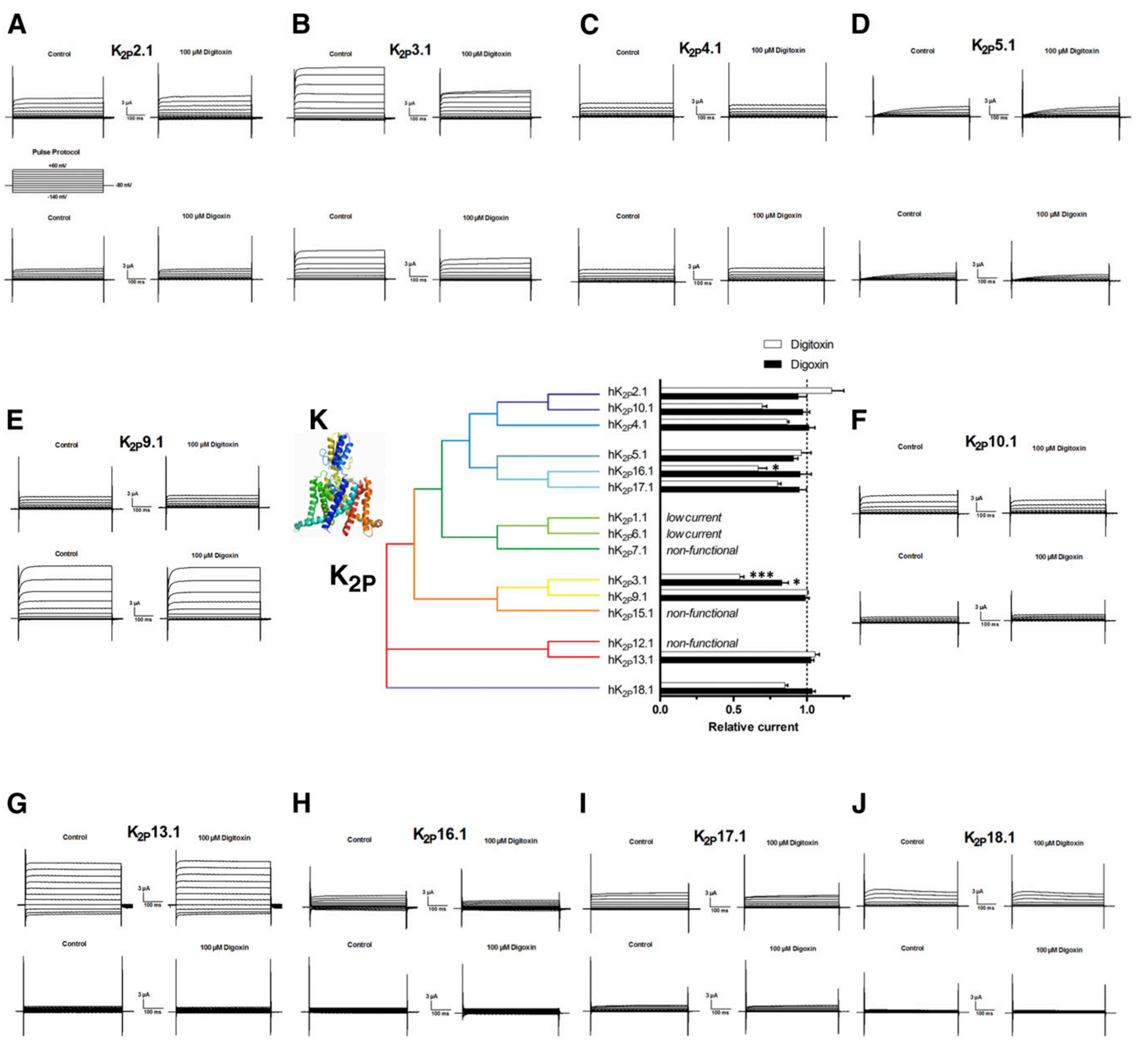

Fig. 1. Effects of digitoxin and digoxin on functional human K_{2P} potassium channels expressed in *Xenopus* oocytes. (A–J) Representative macroscopic currents recorded under control conditions and after 30-minute application of 100 μM digoxin or 100 μM digitoxin are displayed for K_{2P}2.1 (A), K_{2P}3.1 (B), K_{2P}4.1 (C), K_{2P}5.1 (D), K_{2P}9.1 (E), K_{2P}10.1 (F), K_{2P}13.1 (G), K_{2P}16.1 (H), K_{2P}17.1 (I), and K_{2P}18.1 (J), respectively. (K) Currents were quantified at +20 mV membrane voltage. Significant current reduction was observed with human K_{2P}3.1 and K_{2P}16.1 channels. A phylogram of K_{2P}3.1 channel orthologs illustrates the degree of homology between K_{2P} channels. K_{2P} protein sequences were aligned and assembled in a phylogenetic tree view using ClustalW2 software. The three-dimensional homology model of a K_{2P}3.1 channel consisting of two human subunits is based on the crystal structure of human K_{2P}1.1 and K_{2P}4.1 channels. K_{2P}3.1 N and C termini were truncated in the crystal structure-based model consistent with the crystal structure template. Data are given as the mean ± S.E.M. *$P < 0.05$; ***$P < 0.001$ vs. control measurements (n = 3–8 cells).

To our knowledge, the effects of clinically relevant glycosides digoxin and digitoxin on K_{2P} channels have not been assessed to date. This study provides a systematic analysis of digoxin and digitoxin sensitivity among all functional human K_{2P} channels to close this gap. In addition, biophysical mechanisms of K_{2P}3.1 blockade were characterized in detail.

Materials and Methods

Ethics Statement. This study was carried out in accordance with the Guide for the Care and Use of Laboratory Animals as adopted and promulgated by the U.S. National Institutes of Health (publication no. 85-23, revised 1985), and the current version of the German Law on the Protection of Animals was followed. The investigation conforms to Directive 2010/63/EU of the European Parliament. Approval for experiments involving *Xenopus laevis* was granted by the local Animal Welfare Committee (institutional approval numbers A-38/11 and G-221/12).

Molecular Biology. Complementary (c)DNAs encoding human K_{2P}1.1 (GenBank accession number NM_002245), K_{2P}2.1 (EF165334), K_{2P}3.1 (NM_002246), and K_{2P}9.1 (NM_016601) were kindly provided by Steve Goldstein (Chicago, IL). Human K_{2P}18.1 cDNA (NM_181840) was obtained from C. Spencer Yost (San

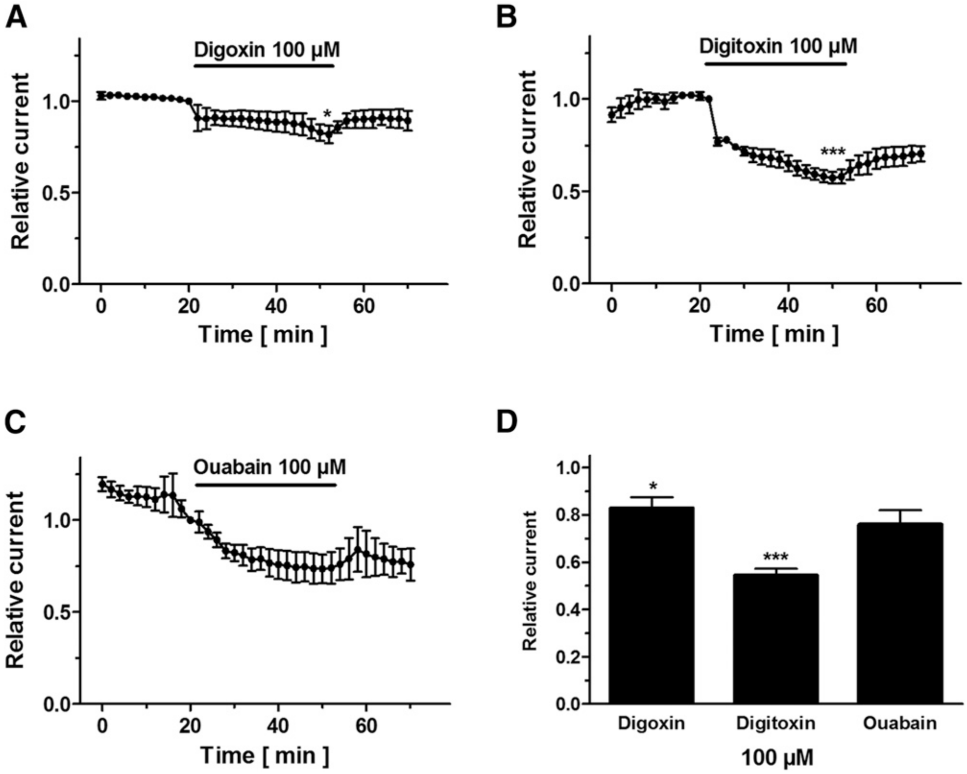

Fig. 2. Comparison between effects of digoxin, digitoxin, and ouabain on $K_{2P}3.1$ currents recorded from *Xenopus* oocytes expressing $K_{2P}3.1$ cRNA. (A–C) Time course of $hK_{2P}3.1$ reduction during application of digoxin (A; $n = 4$), digitoxin (B; $n = 5$), and ouabain (C; $n = 4$). (D) Differential effects of cardiac glycosides on $K_{2P}3.1$ channels. Currents were recorded as described in (A) through (C). Mean ± S.E.M. relative current amplitudes are displayed. *$P < 0.05$; ***$P < 0.001$ vs. control measurements. The *t* tests followed by Bonferroni corrections for multiple testing indicated that differences between glycosides were not statistically significant.

Francisco, CA). Amplification of the following human cDNAs was reported previously: $hK_{2P}4.1$ (EU978935), $K_{2P}5.1$ (EU978936), $K_{2P}6.1$ (EU978937), $K_{2P}10.1$ (EU978939), $K_{2P}13.1$ (EU978942), $K_{2P}16.1$ (EU978943), and $K_{2P}17.1$ (EU978944) (Gierten et al., 2008). Mutations described in this study were introduced with the QuikChange Site-Directed Mutagenesis kit (Stratagene, San Diego, CA) and synthetic mutant oligonucleotide primers. For in vitro transcription, cDNAs were subcloned into dual-purpose expression vectors containing a cytomegalovirus promoter for mammalian expression and a T7 promoter for cRNA synthesis. Plasmids were linearized and transcribed using the T7 mMessage mMachine kit (Ambion, Austin, TX). RNA transcripts were quantified by spectrophotometry after separation by agarose gel electrophoresis.

***X. laevis* Oocyte Preparation.** Ovarian lobes were surgically removed in an aseptic technique from female *X. laevis* frogs anesthetized with 1 g/l tricaine solution (pH 7.5). After collagenase treatment (collagenase A or D; Roche Diagnostics, Mannheim, Germany), stage V to VI defolliculated oocytes were manually isolated under a stereomicroscope. For electrophysiological recordings, complementary (c)RNA (1.5–12.5 ng; 46 nl/oocyte) encoding study channels was injected.

Electrophysiology. Two-electrode voltage clamp measurements were performed to record whole cell currents from *X. laevis* oocytes 1–5 days after cRNA injection. Two-electrode voltage clamp electrodes were pulled from 1-mm borosilicate glass tubes (Science Products, Hofheim, Germany) using a P-87 micropipette puller (Sutter Instruments, Novato, CA). Macroscopic currents were recorded using an OC-725C Oocyte Clamp amplifier (Warner Instruments, Hamden, CT) and pClamp software (Molecular Devices, Sunnyvale, CA). Data were sampled at 2 kHz and low-pass filtered at 1 kHz. Leak currents were not subtracted. Current amplitudes were determined at the end of +20-mV voltage pulses unless stated otherwise. Voltage clamp measurements were carried out at room temperature (20–22°C). Voltage clamp electrodes filled with 3 M KCl solution had tip resistances of 1.5–3 MΩ. Experiments were performed under constant perfusion by a gravity-driven perfusion system. The standard extracellular bath solution contained 96 mM NaCl, 4 mM KCl, 1.1 mM $CaCl_2$, 1 mM $MgCl_2$, and 5 mM HEPES. The pH was adjusted with NaOH to pH 7.4. Human $K_{2P}16.1$ and $K_{2P}17.1$ currents were activated by adjusting the extracellular pH to 8.5 (Gierten et al., 2008).

Drugs. Digoxin, digitoxin, and ouabain (Prassas and Diamandis, 2008) were obtained from Sigma-Aldrich (Steinheim, Germany) and dissolved in dimethylsulfoxide to 100 mM stock solutions. Stock solutions were stored at −20°C. Aliquots of the stock solutions were diluted to the desired concentration with the bath solution on the day of experiments. The solvent (0.1% dimethylsulfoxide; 30 minutes) did not significantly affect mean $K_{2P}3.1$, $K_{2P}6.1$, or $K_{2P}16.1$ current amplitudes (data not shown).

Data and Statistical Analyses. PCLAMP (Axon Instruments, Foster City, CA), Origin 8 (OriginLab, Northampton, MA), Prism 6.0 (GraphPad Software Inc., La Jolla, CA), and Excel (Microsoft, Redmond, WA) software were used for data acquisition and analysis. Concentration-response relationships for drug-induced block were fit with a Hill equation of the following form: $I_{drug}/I_{control} = 1/[1 + (D/IC_{50})^n]$, where *I* indicates current, D is the drug concentration, n is the Hill coefficient, and IC_{50} is the concentration necessary for 50% block. Data are expressed as the mean ± S.E.M. Paired and unpaired *t* tests (two-tailed tests) were applied to compare the statistical significance of the results. $P < 0.05$ was considered statistically significant. Multiple comparisons were performed using one-way analysis of variance. If the hypothesis of equal means could be rejected at the 0.05 level, pairwise comparisons of groups were made and the probability values were adjusted for multiple comparisons using the Bonferroni correction.

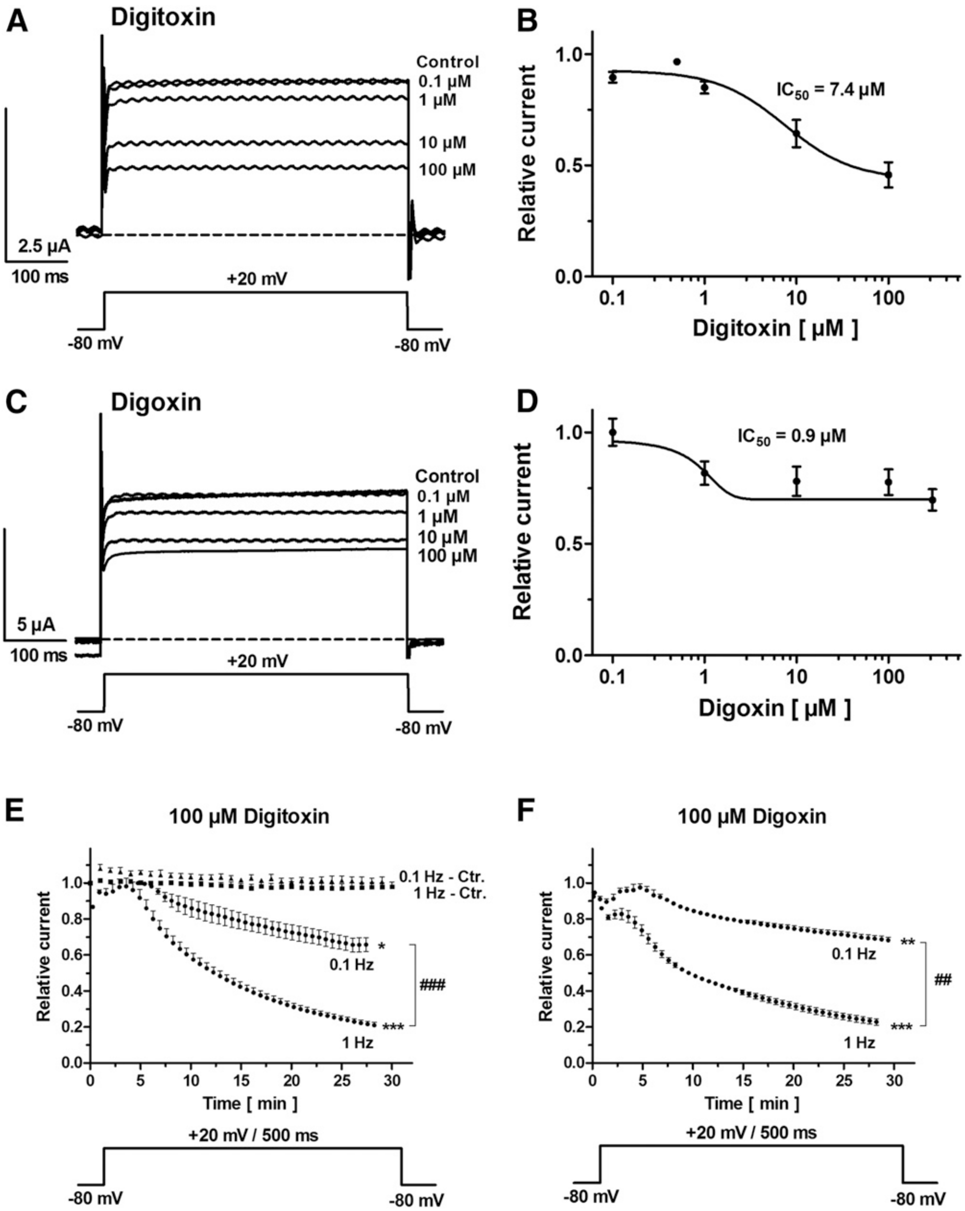

Fig. 3. Concentration-dependent effects of digoxin and digitoxin on $K_{2P}3.1$ currents. (A and C) Representative macroscopic $hK_{2P}3.1$ currents recorded under control conditions and after 30-minute application of indicated concentrations of digitoxin (A) or digoxin (C) are shown. Dashed lines indicate zero current level. (B and D) Concentration-response relationships for the effects of digitoxin (B) and digoxin (D) on $hK_{2P}3.1$ outward currents measured at the end of the +20 mV voltage step (n = 3–6 cells). The IC_{50} values yielded 7.4 μM (digitoxin) and 0.9 μM (digoxin). (E and F) Block of $K_{2P}3.1$ is frequency dependent. Mean relative $K_{2P}3.1$ current amplitudes recorded at +20 mV membrane potential (1- and 0.1-Hz stimulation rate) are plotted versus time (n = 4 oocytes were studied at each rate; error bars denote the S.E.M.). $^{*}P < 0.05$; $^{**}P < 0.01$; $^{***}P < 0.001$ vs. control conditions; $^{\#\#}P < 0.01$; $^{\#\#\#}P < 0.001$ vs. 0.1 Hz. In addition, current amplitudes obtained during 30 minutes in drug-free solution at 1-Hz (1 Hz – Ctr.; n = 6) and 0.1-Hz stimulation rates (0.1 Hz – Ctr.; n = 6) are shown. For the purposes of clear presentation, not all measurements are displayed.

Results

Effects of Cardiac Glycosides on Human K_{2P} K^+ Channels. Pharmacological effects of cardiac glycosides digoxin and digitoxin on all functional human K_{2P} channels were assessed using the *X. laevis* oocyte expression system. From a holding potential of −80 mV, currents were activated using test pulses (500 milliseconds) to voltages between −140 and +60 mV in 20-mV increments. Human $K_{2P}1.1$ and $K_{2P}6.1$ subunits produced very low current amplitudes that did not allow for reasonable pharmacology testing. Inhibitory effects of 100 μM digoxin or digitoxin (30-minute incubation) on K_{2P} family members are summarized in Fig. 1. Digitoxin significantly inhibited human K_{2P} channels 3.1 (−45.6% ± 6.3%; n = 5; P < 0.0001) and 16.1 (−33.2% ± 10.0%; n = 4; P = 0.029). We observed reduced $K_{2P}3.1$ currents after application of digoxin as well (−17.1% ± 10.2%; n = 5; P = 0.020). The time course of effect is shown in Fig. 2, A and B. After a control period with no significant amplitude changes (20 minutes), $K_{2P}3.1$ currents decreased rapidly upon administration of 100 μM digoxin (Fig. 2A) or 100 μM digitoxin (Fig. 2B). Inhibitory effects of digitoxin and digoxin were partially reversible. Current levels reached 89.4% ± 12.2% (digoxin; n = 5) and 68.5% ± 0.2% (digitoxin; n = 5) of control amplitudes 20 minutes after removal of the drug. Blockade of $K_{2P}3.1$ channels remained incomplete, with maximum current reduction of 17.1% (digoxin) and 45.6% (digitoxin) in oocytes (Fig. 2, A, B, and D), a finding similar to inhibition of $K_{2P}2.1$ (carvedilol, dronedarone) or $K_{2P}3.1$ (amiodarone, dronedarone) channels reported earlier (Gierten et al., 2010; Schmidt et al., 2012; Kisselbach et al., 2014). To probe the specificity of the pharmacological action of digoxin and digitoxin on $K_{2P}3.1$ among cardiac glycosides, we studied the effects of ouabain (100 μM) under similar experimental conditions. Application of ouabain reduced $hK_{2P}3.1$ currents

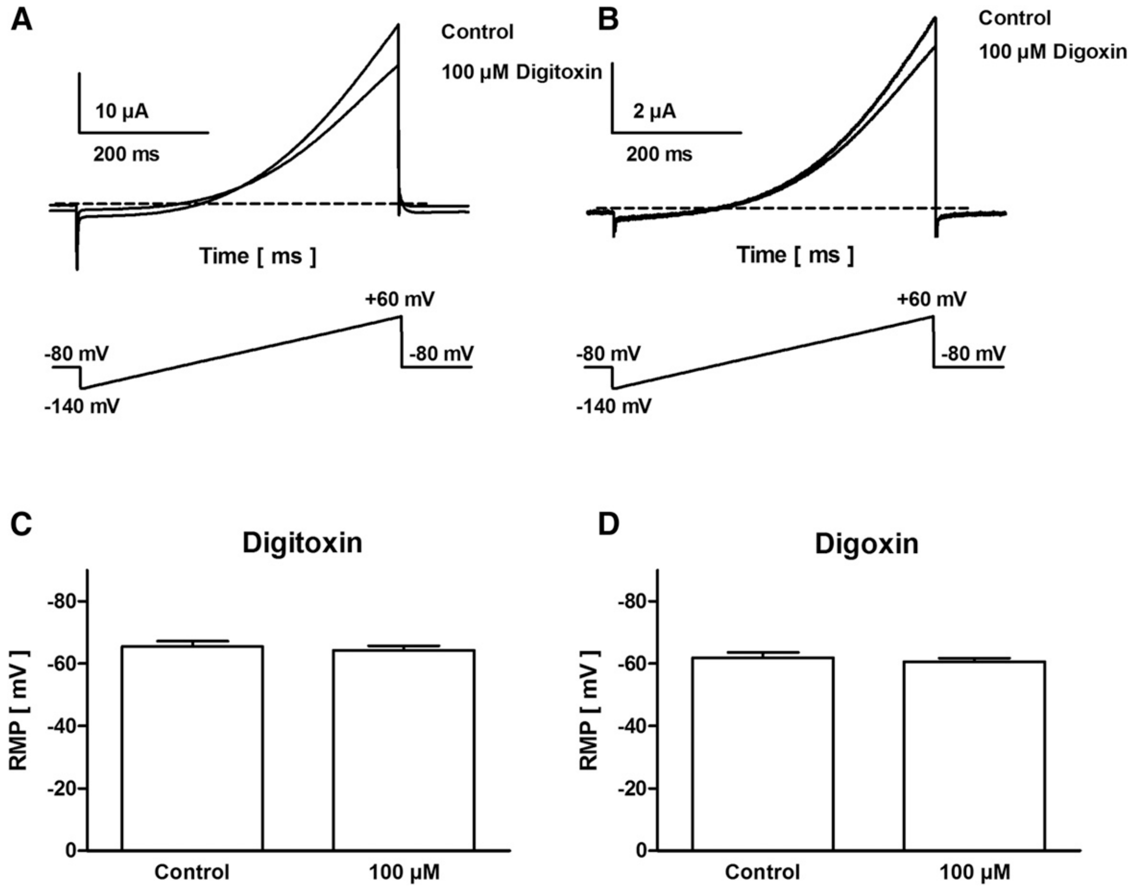

Fig. 4. Effects of cardiac glycosides on outward rectification and resting membrane potentials. (A and B) Outward rectification of $K_{2P}3.1$ currents elicited by voltage ramps from −140 to +60 mV. Typical recordings from the same cell in the absence of the drug and after 30-minute superfusion with 100 μM digitoxin (A) or 100 μM digoxin (B) are superimposed. Dashed lines indicate zero current level. (C and D) Mean resting membrane potentials (RMPs) of *Xenopus* oocytes, measured before and after blockade of $K_{2P}3.1$ with digitoxin (C; 100 μM, 30 minutes; n = 5) or digoxin (D; 100 μM, 30 minutes; n = 5). Data are given as the mean ± S.E.M.

(−28.7% ± 13.5%), albeit without reaching statistical significance (n = 5; P = 0.07) (Fig. 2, C and D).

Inhibition of $K_{2P}3.1$ Channels by Digitoxin and Digoxin. Pharmacological actions of digitoxin and digoxin on human $K_{2P}3.1$ channels were studied in detail. Channels expressed in oocytes were activated as described in Fig. 1 and quantified at +20 mV after drug administration for 30 minutes (Fig. 3, A and C). Currents in the presence of the drug were normalized to their respective control values and plotted as relative current amplitudes (Fig. 3, B and D). Digitoxin and digoxin reduced $K_{2P}3.1$ potassium currents in a concentration-dependent manner. The IC_{50} values for blockade of $K_{2P}3.1$ channels yielded 7.4 μM (digitoxin; Hill coefficient n_H = 1.2; n = 3–6 cells; Fig. 3B) and 0.9 μM (digoxin; n_H = 2.0; n = 3–6; Fig. 3D).

To study the frequency dependence of block, $K_{2P}3.1$ currents were rapidly activated by a depolarizing step to +20 mV (500 milliseconds) at intervals of 1 or 10 seconds, respectively. The development of current reduction in the presence of 100 μM digitoxin (Fig. 3E) or 100 μM digoxin (Fig. 3F) was plotted against time. Blockade of $K_{2P}3.1$ channels by cardiac glycosides was frequency dependent. The degree of inhibition after 30-minute digitoxin application was significantly (P = 0.0004) higher at the 1-Hz stimulation rate (79.7% ± 2.5%; n = 4; P = 0.0003) compared with 0.1 Hz (34.3% ± 6.9%; n = 4; P = 0.013). Similar to digitoxin, inhibition by digoxin displayed frequency dependence with more pronounced blockade (P = 0.0005) at 1-Hz (77.8% ± 3.1%; n = 4; P = 0.0005) than at 0.1-Hz (32.3% ± 3.1%; n = 4; P = 0.003) stimulation rates. $K_{2P}3.1$ currents recorded in drug-free solution were stable during rapid activation at 1 Hz (n = 6) or 0.1 Hz (n = 6) for 30 minutes, respectively (Fig. 3E).

Biophysical Analysis of $K_{2P}3.1$ Inhibition by Cardiac Glycosides. $K_{2P}3.1$ currents exhibited electrophysiological characteristics typical for a potassium-selective background leak conductance, that is, a voltage-independent portal showing Goldman-Hodgkin-Katz (outward) rectification. To assess the effects of digoxin and digitoxin on $K_{2P}3.1$ rectification, linear ramp voltage protocols were applied between −140 and +60 mV (500 milliseconds) before and after drug application for 30 minutes (Fig. 4, A and B). Outward rectification was observed before and after digitoxin (n = 5) and digoxin application (n = 5). The degree of block determined at +20 mV ramp potential was 19.5% ± 0.4% (n = 3; P = 0.005) for digitoxin and 10.3% ± 22.5% (n = 3; P = 0.15) for digoxin. Moderate reduction of $K_{2P}3.1$ leak currents by glycosides was not associated with significant changes in the resting membrane potential (Fig. 4, C and D).

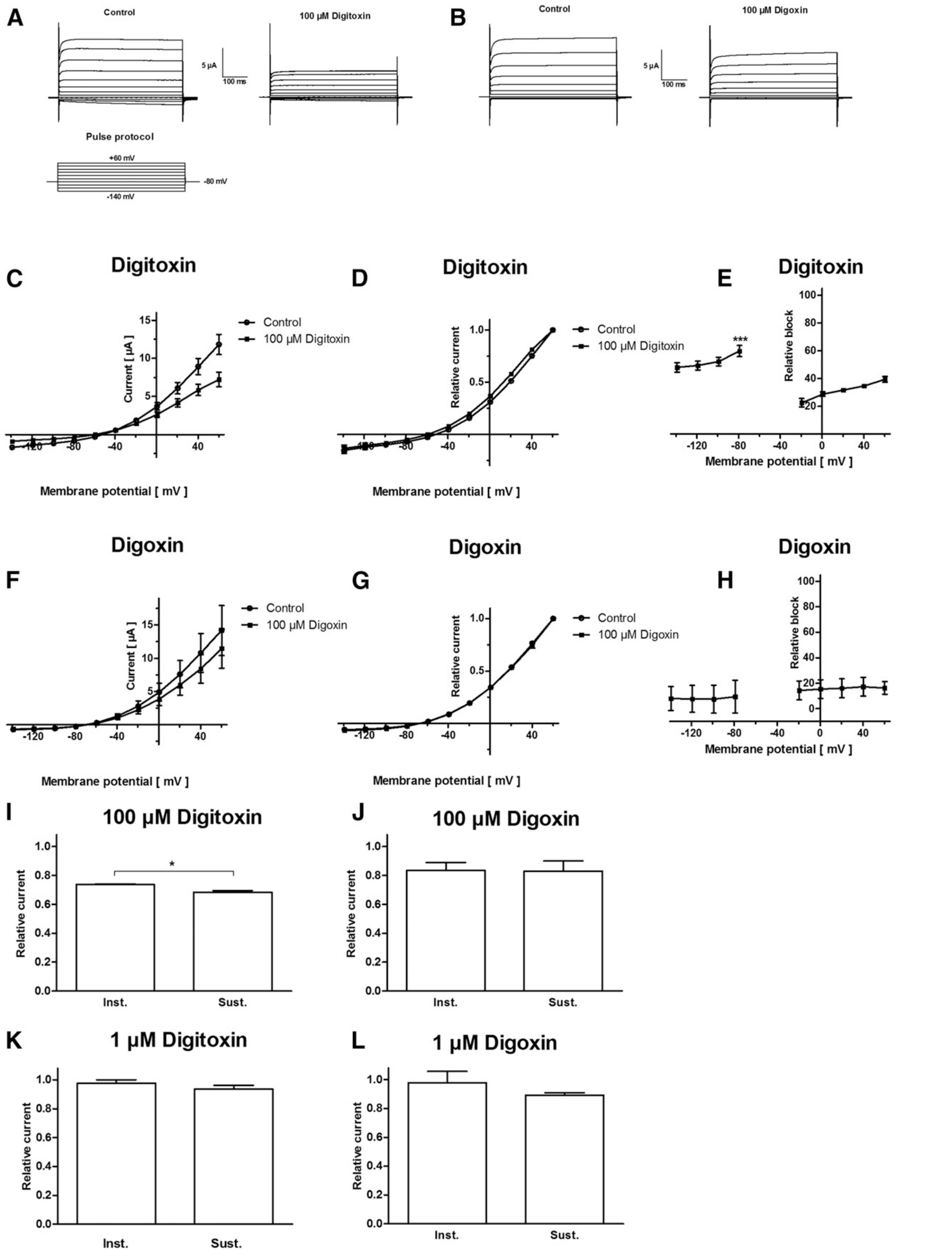

Fig. 5. Biophysical characteristics of K_{2P}3.1 channel blockade by digitoxin and digoxin. (A–H) Effects of cardiac glycosides on K_{2P}3.1 voltage dependence of activation. Control measurements and the effects of 100 μM digitoxin (A; 30 minutes) or digoxin (B; 30 minutes) are shown in representative oocytes. (C, D, F, and G) Activation curves (i.e., step current amplitudes as a function of test potentials) recorded under isochronal conditions (C and F: original current amplitudes; D and G: values normalized to maximum currents). (E and H) Fraction of blocked step currents, plotted as function of the respective test pulse potential (digitoxin, n = 12; digoxin, n = 11). ***$P < 0.001$, −80 mV versus −20 mV. (I and J) Digitoxin (I; 100 μM, n = 6) and digoxin

Drug effects on $K_{2P}3.1$ current-voltage (*I-V*) relationships were investigated under isochronal recording conditions. From a holding potential of −80 mV, pulses were applied for 500 milliseconds to voltages between −140 and +60 mV in 20-mV increments (0.2 Hz). Representative current traces are shown for control conditions and after application of 100 μM digitoxin (30 minutes; Fig. 5A) and 100 μM digoxin (30 minutes; Fig. 5B). The current-voltage relationships were not affected by drug administration (Fig. 5, C, D, F, and G). Relative inhibition of $K_{2P}3.1$ currents was plotted as a function of the test pulse potential in Fig. 5E (digitoxin; $n = 7$) and Fig. 5H (digoxin; $n = 7$), revealing an attenuation of current inhibition by digitoxin at more depolarized test potentials (−80 vs. −20 mV; $P = 0.0001$).

$K_{2P}3.1$ channels activate in two phases. The currents activate quickly to approximately 85% of their respective maximum amplitudes within approximately 50 milliseconds, followed by a markedly slower additional activation time course. Thus, macroscopic $K_{2P}3.1$ currents may be divided into an instantaneous (measured 2 milliseconds after the step to +20 mV) and a time-dependent current component (measured at the end of the 500-millisecond test pulse), respectively. The instantaneous current was 80.5% ± 14.4% of the fully activated current under control conditions ($n = 5$) prior to digitoxin administration. Before digoxin exposure, instantaneous control currents yielded 77.6% ± 27.8% of maximum currents ($n = 5$). Inhibition of the sustained component by 100 μM digitoxin (30 minutes) (31.6% ± 2.8% current reduction) was stronger compared with the instantaneous current (26.3% ± 0.8% inhibition; $P = 0.011$; Fig. 5I). By contrast, effects of digoxin on instantaneous current (−16.6% ± 12.2%) and on fully activated current (−17.0% ± 15.6%) were similar ($n = 5$; $P = 0.97$) (Fig. 5J). In addition, time-dependent channel activation was investigated in the presence of low digitoxin concentrations. To this end, 1 μM digitoxin or 1 μM digoxin was applied for 30 minutes, and currents were measured at +20 mV at the indicated 2 and 500 milliseconds, respectively. The instantaneous current was 81.5% ± 2.2% of the fully activated current under control conditions ($n = 5$) prior to digitoxin administration in this set of experiments. Before digoxin exposure, instantaneous control currents yielded 75.2% ± 2.0% of maximum currents ($n = 3$). Inhibition of the sustained component by 1 μM digitoxin (5.6% ± 2.8% current reduction) was low and did not differ from instantaneous current block (2.4% ± 2.4% inhibition; $n = 4$ to 5; $P = 0.29$; Fig. 5K). Similarly, effects of digoxin on instantaneous current (−10.8% ± 1.7%) and on fully activated current (−2.2% ± 8.0%) were not significantly different ($n = 3$; $P = 0.39$) (Fig. 5L).

Structural Determinants of Glycoside Binding to $K_{2P}3.1$ Channels. Prior mutagenesis and docking studies of $K_{2P}3.1$ (Fig. 6, A–C) and related $K_{2P}9.1$ channels that show virtually identical pore regions (Fig. 6D) indicated that amino acid residue L122 in the M2 domain and residues I235, G236, and L239 in the M4 domain contribute to hydrophobicity of the $K_{2P}3.1$ pore and affect drug binding (Streit et al., 2011; Chokshi et al., 2015). In addition, N240 and other residues with side chains directed away from the pore reduced drug sensitivity of the channels, possibly via indirect effects on pore access or gating (Streit et al., 2011; Chokshi et al., 2015). We investigated effects of digitoxin and digoxin on mutant $K_{2P}3.1$-L122A, $K_{2P}3.1$-I235A, $K_{2P}3.1$-G236A, $K_{2P}3.1$-L239A, and $K_{2P}3.1$-N240A channels to assess the significance of these amino acid residues in glycoside blockade of $K_{2P}3.1$. The effects of eliminating an aromatic F residue at position 238 on drug binding were studied as well ($K_{2P}3.1$-F238A). The voltage protocol described in Fig. 1 was applied to activate $K_{2P}3.1$ channels, and amplitudes were quantified at +20 mV. Currents were recorded under control conditions, followed by application of 100 μM digitoxin or digoxin for 30 minutes (Fig. 6, E–J). Cardiac glycosides reduced $K_{2P}3.1$ wild-type currents by 45.6% ± 6.3% (digitoxin; $n = 5$; $P < 0.0001$; Fig. 6K) and by 17.1% ± 10.2% (digoxin; $n = 5$; $P = 0.020$; Fig. 6L). By contrast, inhibitory effects of digitoxin and digoxin were attenuated or prevented by replacement of amino acids L122, I235, G236, F238, L239, and N240 with alanine residues (Fig. 6, K and L). Inhibition in the presence of digitoxin yielded 3.0% ± 3.6% (L122A; $n = 5$), 23.0% ± 12.6% (I235A; $n = 5$), 24.3% ± 9.0% (G236A; $n = 5$), 2.1% ± 4.6% (F238A; $n = 3$), 2.1% ± 3.6% (L239A; $n = 3$), and +5.6% ± 7.5% (N240A; $n = 5$). After digoxin application, current block yielded 0.0% ± 4.4% (L122A; $n = 5$), 10.5% ± 5.0% (I235A; $n = 5$), 18.8% ± 3.0% (G236A; $n = 3$), +3.8% ± 13.1% (F238A; $n = 3$), +2.3% ± 7.7% (L239A; $n = 4$), and +2.4% ± 6.0% (N240A; $n = 5$).

Discussion

Cardiac K_{2P} Background K^+ Currents Are Inhibited by Digoxin and Digitoxin. Digitoxin blocked human cardiac K_{2P} channels $K_{2P}3.1$ and $K_{2P}16.1$. By contrast, digoxin selectively inhibited $K_{2P}3.1$ channels, whereas other K_{2P} channels were fully insensitive to the drug. Thus, multichannel K_{2P} blocking properties are specific to digitoxin and distinguish it from digoxin. $K_{2P}16.1$ channels exhibit negligible expression in the human heart (Schmidt et al., 2015), indicating little significance of $K_{2P}16.1$ inhibition by digitoxin. The primary mechanism of glycoside action is assumed to be directly related to inhibition of Na^+/K^+-ATPase function that increases intracellular Na^+ levels, which translate into elevated intracellular Ca^{2+} concentrations via the Na^+/Ca^{2+} exchanger (Altamirano et al., 2006). However, these actions occur at very high concentrations, challenging this reasoning. Further electrophysiological actions comprise inhibition of human ether-a-go-go K^+ channel trafficking and the mediation of calcium entry into cells by forming ion channels (Wang et al., 2007; Arispe et al., 2008). Targeting of

(J; 100 μM, $n = 7$) blockade of the sustained (Sust.) current component of $K_{2P}3.1$ was more pronounced compared with the instantaneous (Inst.) current. (K and L) Inhibition of instantaneous and sustained current components was not significantly different in the presence of lower digitoxin (K; 1 μM, $n = 4$ to 5) and digoxin (L; 1 μM, $n = 3$) concentrations. Data are provided as the mean ± S.E.M. *$P < 0.05$.

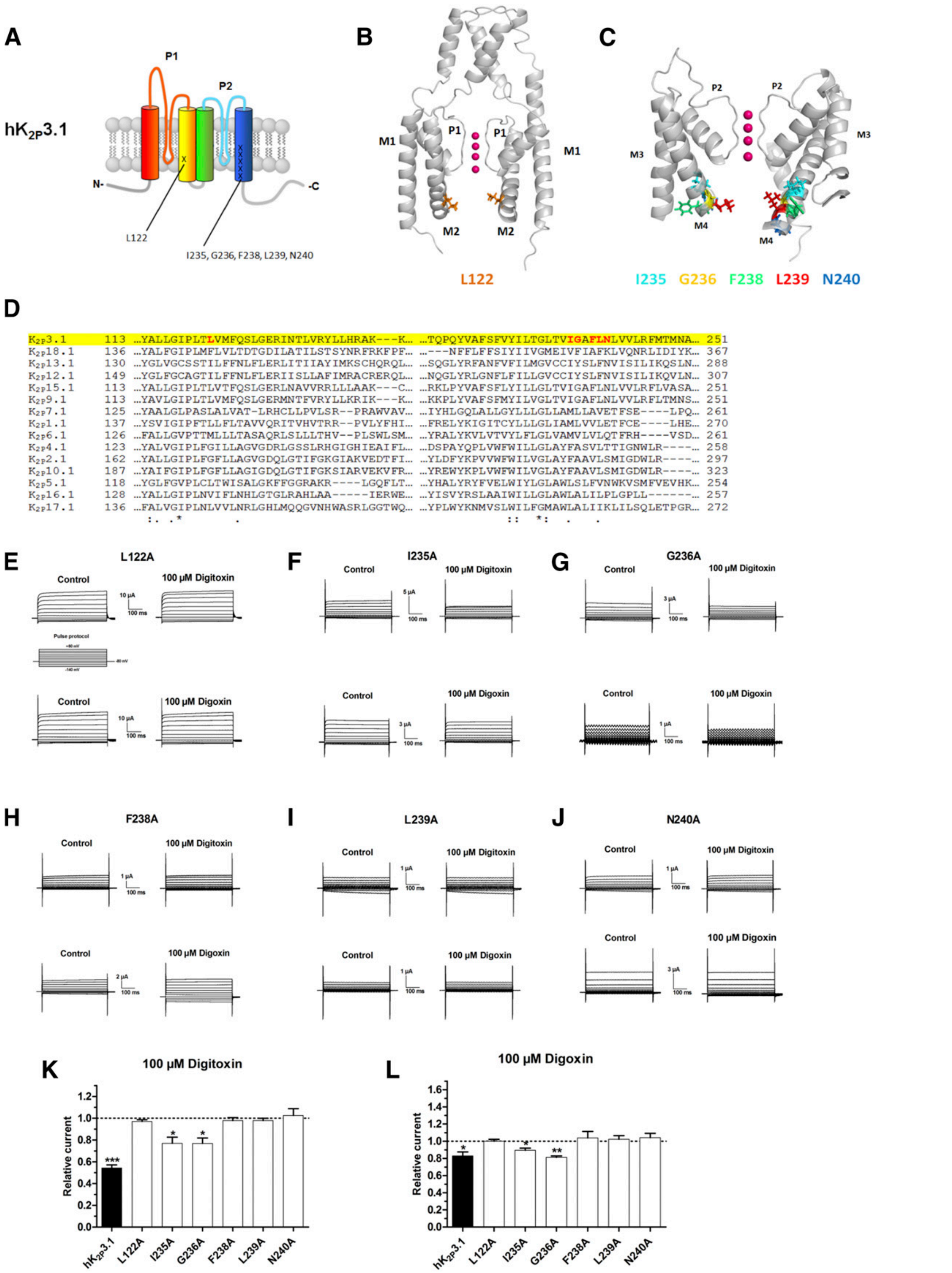

Fig. 6. Molecular determinants of drug binding to $K_{2P}3.1$ channels. (A) Hypothetical, two-dimensional membrane model of a $K_{2P}3.1$ monomer shows four transmembrane (M) domains and two-pore-forming loops (P) arranged in tandem. Amino acid residues located at the cytoplasmic region of pore helices 2 and 4 and predicted to affect drug binding are highlighted. (B and C) Three-dimensional homology models of M1-P1-M2 (B) and M3-P2-M4 regions (C) of dimeric $K_{2P}3.1$ channels illustrate the location of residues investigated here. Pink circles indicate K^+ ions inside the selectivity filter. Models were based on the crystal structures of $K_{2P}1.1$ (PDB ID, 3UKM) and $K_{2P}4.1$ channels (PBD ID, 3UM7). (D) Amino acid sequence alignments of

K_{2P} currents extends the electrophysiological profile of digoxin and digitoxin. Furthermore, molecular and biophysical analyses performed in this study provide mechanistic insights into K_{2P} channel pharmacology that are required for the evaluation of this emerging ion channel family as a future drug target.

The Biophysical Mechanism of K_{2P}3.1 Channel Inhibition by Digitoxin. The rapid onset of block supports a direct digoxin-channel interaction as opposed to increased K_{2P}3.1 protein turnover or accelerated channel degradation as a molecular mechanism of action. Concentration-dependent digoxin block of K_{2P}3.1 was characterized by a Hill coefficient n_H of 2, suggesting cooperative binding. By contrast, no cooperativity of binding was noted with digitoxin (n_H = 1.2). Higher digoxin binding efficiency at a single ion channel compared with digitoxin may have contributed to the lack of K_{2P}3.1 activation slowing that was present only when low digitoxin concentrations were applied. Outward rectification that is characteristic to K_{2P}3.1 channel function in physiologic ionic conditions was similarly observed before and during drug block. K_{2P}3.1 channels were blocked at hyperpolarized and depolarized membrane potentials. Incomplete K_{2P}3.1 current inhibition may be attributed to specific lipophilic properties of the oocyte expression system. Unblocking occurred slowly, and a complete washout could not be achieved. The lack of full reversibility may be attributed to trapping of digitoxin molecules in the K_{2P}3.1 channel pore. This notion is supported by reduced affinity to digitoxin after mutation of amino acid residues L122, I235, G236, F238, L239, and N240 that are located at the cytoplasmic face of the K_{2P}3.1 channel pore and constitute parts of a drug binding site (Streit et al., 2011; Chokshi et al., 2015). In addition, intracellular accumulation of the drug may have contributed to slow washout kinetics. Finally, slow unblocking kinetics resulted in frequency-dependent accumulation of K_{2P}3.1 block.

Clinical Implications. K^+ channel block exerts class III antiarrhythmic action, suppressing cardiac arrhythmia through prolongation of cardiomyocyte APD and prevention of electrical reentry. Thus, K_{2P} K^+ current blockade described in this study could contribute to cardiac electrophysiological effects of cardiac glycosides. To evaluate the physiologic significance of pharmacological in vitro effects, a comparison of concentration-response relationships with therapeutic plasma levels of the drugs is required. Digitoxin blocked hK_{2P}3.1 channels with an IC_{50} value of 7.4 μM, whereas digoxin achieved only weak K_{2P}3.1 current inhibition even at high concentrations (100 μM). Digitoxin plasma concentrations between 20 and 30 nM were reached in patients and exceeded under conditions of intoxication, whereas digoxin levels only ranged from 1 to 2 nM (Wang et al., 2007). Given the marked difference between plasma levels and concentrations required for channel block in vitro, we conclude that little electrophysiological effects of K_{2P}3.1 current inhibition might be expected during routine therapeutic use of digoxin and digitoxin. This is in line with cellular effects of cardiac glycosides on APD. In contrast to APD prolongation expected for K^+ channel blockers, digoxin induces biphasic effects on cardiac APD, characterized by initial prolongation followed by marked APD shortening during drug application in vitro (Mandel et al., 1972). APD shortening has been reported for digitoxin as well (Lüllmann et al., 1983).

Nonetheless, the data revealed here may support the development of differential antiarrhythmic therapy against complex and heterogenous mechanisms of AF. The "classical" mechanism of atrial arrhythmogenesis in AF involves increased atrial K^+ currents, resulting in shortening of APD and effective refractory periods that perpetuate AF through the promotion of electrical reentry (Schmidt et al., 2011). This mechanism is observed in patients with persistent or permanent AF (Schmidt et al., 2015, 2017). In these cases, inhibition of repolarizing K_{2P}3.1 currents that are selectively expressed in human atrium may be effective to suppress AF. We conclude that mechanistic and biophysical information on K_{2P}3.1 channel inhibition by digitoxin constitutes a starting point for the development of future, K_{2P}-based antiarrhythmic paradigms.

In conclusion, K_{2P} current inhibition by cardiac glycosides represents a previously unrecognized mode of action that extends the electrophysiological profile of the drugs and provides mechanistic evidence to further confirm cardiac K_{2P} channels as antiarrhythmic drug targets in general. This is particularly significant, as comprehensive knowledge of the molecular mechanism of action may be critical for clinical application safety. The clinical antiarrhythmic significance of K_{2P} current blockade by digoxin and digitoxin in heart rhythm disorders requires validation in translational and clinical investigations.

Acknowledgments

The authors acknowledge the excellent technical support of Simone Bauer, Katrin Kupser, Kai Sona, and Nadine Weiberg.

Authorship Contributions

Participated in research design: Schmidt, Wiedmann, Thomas.

Conducted experiments: Schmidt, Wiedmann, Gaubatz, Ratte.

Performed data analysis: Schmidt, Wiedmann, Gaubatz, Ratte, Thomas.

Wrote or contributed to the writing of the manuscript: Schmidt, Wiedmann, Gaubatz, Ratte, Katus, Thomas.

pore regions 1 and 2 of K_{2P}3.1 (highlighted in yellow) and other K_{2P} family members. Amino acid residues predicted to affect drug binding to the pore are marked in red. (E–J) Acute effects of 100 μM digitoxin and 100 μM digoxin (30 minutes) on mutant K_{2P}3.1-L122A (E), K_{2P}3.1-I235A (F), K_{2P}3.1-G236A (G), K_{2P}3.1-F238A (H), K_{2P}3.1-L239A (I), and K_{2P}3.1-N240A channels (J). (K and L) Mean relative outward current amplitudes measured at +20 mV for K_{2P}3.1 wild type ($n_{digitoxin}$ = 6; $n_{digoxin}$ = 6), K_{2P}3.1-L122A ($n_{digitoxin}$ = 5; $n_{digoxin}$ = 5), K_{2P}3.1-I235A ($n_{digitoxin}$ = 5; $n_{digoxin}$ = 6), K_{2P}3.1-G236A ($n_{digitoxin}$ = 5; $n_{digoxin}$ = 5), K_{2P}3.1-F238A ($n_{digitoxin}$ = 4; $n_{digoxin}$ = 5), K_{2P}3.1-L239A ($n_{digitoxin}$ = 5; $n_{digoxin}$ = 5), and K_{2P}3.1-N240A ($n_{digitoxin}$ = 5; $n_{digoxin}$ = 5), respectively. Inhibitory effects of digitoxin and digoxin were prevented by pore region mutations. *P < 0.05; **P < 0.01; ***P < 0.001 versus respective control recordings (see the text for voltage protocols). PDB ID, Protein Data Bank identifier; WT, wild type.

References

Altamirano J, Li Y, DeSantiago J, Piacentino V, 3rd, Houser SR, and Bers DM (2006) The inotropic effect of cardioactive glycosides in ventricular myocytes requires Na+-Ca2+ exchanger function. *J Physiol* **575**:845–854.

Arispe N, Diaz JC, Simakova O, and Pollard HB (2008) Heart failure drug digitoxin induces calcium uptake into cells by forming transmembrane calcium channels. *Proc Natl Acad Sci USA* **105**:2610–2615.

Bavendiek U, Aguirre Davila L, Koch A, and Bauersachs J (2017) Assumption versus evidence: the case of digoxin in atrial fibrillation and heart failure. *Eur Heart J* **38**: 2095–2099.

Chai S, Wan X, Nassal DM, Liu H, Moravec CS, Ramirez-Navarro A, and Deschênes I (2017) Contribution of two-pore K^+ channels to cardiac ventricular action potential revealed using human iPSC-derived cardiomyocytes. *Am J Physiol Heart Circ Physiol* **312**:H1144–H1153.

Chokshi RH, Larsen AT, Bhayana B, and Cotten JF (2015) Breathing stimulant compounds inhibit TASK-3 potassium channel function likely by binding at a common site in the channel pore. *Mol Pharmacol* **88**:926–934.

Donner BC, Schullenberg M, Geduldig N, Hüning A, Mersmann J, Zacharowski K, Kovacevic A, Decking U, Aller MI, and Schmidt KG (2011) Functional role of TASK-1 in the heart: studies in TASK-1-deficient mice show prolonged cardiac repolarization and reduced heart rate variability. *Basic Res Cardiol* **106**:75–87.

Gierten J, Ficker E, Bloehs R, Schlömer K, Kathöfer S, Scholz E, Zitron E, Kiesecker C, Bauer A, Becker R, et al. (2008) Regulation of two-pore-domain (K_{2P}) potassium leak channels by the tyrosine kinase inhibitor genistein. *Br J Pharmacol* **154**: 1680–1690.

Gierten J, Ficker E, Bloehs R, Schweizer PA, Zitron E, Scholz E, Karle C, Katus HA, and Thomas D (2010) The human cardiac K_{2P}3.1 (TASK-1) potassium leak channel is a molecular target for the class III antiarrhythmic drug amiodarone. *Naunyn Schmiedebergs Arch Pharmacol* **381**:261–270.

Goldstein SA, Bockenhauer D, O'Kelly I, and Zilberberg N (2001) Potassium leak channels and the *KCNK* family of two-P-domain subunits. *Nat Rev Neurosci* **2**: 175–184.

Hancox JC, James AF, Marrion NV, Zhang H, and Thomas D (2016) Novel ion channel targets in atrial fibrillation. *Expert Opin Ther Targets* **20**:947–958.

Kirchhof P, Benussi S, Kotecha D, Ahlsson A, Atar D, Casadei B, Castella M, Diener HC, Heidbuchel H, Hendriks J, et al.; ESC Scientific Document Group (2016) 2016 ESC guidelines for the management of atrial fibrillation developed in collaboration with EACTS. *Eur Heart J* **37**:2893–2962.

Kisselbach J, Seyler C, Schweizer PA, Gerstberger R, Becker R, Katus HA, and Thomas D (2014) Modulation of K_{2P} 2.1 and K_{2P} 10.1 $K^{(+)}$ channel sensitivity to carvedilol by alternative mRNA translation initiation. *Br J Pharmacol* **171**: 5182–5194.

Lüllmann H, Niehus U, Pulss W, and Ravens U (1983) Electrophysiological studies of some semisynthetic cardiac glycoside derivatives in isolated papillary muscle of the guinea-pig. *Br J Pharmacol* **79**:755–764.

Mandel WJ, Bigger JT, Jr, and Butler VP, Jr (1972) The electrophysiologic effects of low and high digoxin concentrations on isolated mammalian cardiac tissue: reversal by digoxin-specific antibody. *J Clin Invest* **51**:1378–1387.

Prassas I and Diamandis EP (2008) Novel therapeutic applications of cardiac glycosides. *Nat Rev Drug Discov* **7**:926–935.

Ravens U (2010) Novel pharmacological approaches for antiarrhythmic therapy. *Naunyn Schmiedebergs Arch Pharmacol* **381**:187–193.

Schmidt C, Kisselbach J, Schweizer PA, Katus HA, and Thomas D (2011) The pathology and treatment of cardiac arrhythmias: focus on atrial fibrillation. *Vasc Health Risk Manag* **7**:193–202.

Schmidt C, Wiedmann F, Schweizer PA, Becker R, Katus HA, and Thomas D (2012) Novel electrophysiological properties of dronedarone: inhibition of human cardiac two-pore-domain potassium (K_{2P}) channels. *Naunyn Schmiedebergs Arch Pharmacol* **385**:1003–1016.

Schmidt C, Wiedmann F, Schweizer PA, Katus HA, and Thomas D (2014) Inhibition of cardiac two-pore-domain K^+ (K_{2P}) channels–an emerging antiarrhythmic concept. *Eur J Pharmacol* **738**:250–255.

Schmidt C, Wiedmann F, Voigt N, Zhou XB, Heijman J, Lang S, Albert V, Kallenberger S, Ruhparwar A, Szabó G, et al. (2015) Upregulation of K(2P)3.1 K^+ current causes action potential shortening in patients with chronic atrial fibrillation. *Circulation* **132**:82–92.

Schmidt C, Wiedmann F, Zhou XB, Heijman J, Voigt N, Ratte A, Lang S, Kallenberger SM, Campana C, Weymann A, et al. (2017) Inverse remodelling of K_{2P}3.1 K^+ channel expression and action potential duration in left ventricular dysfunction and atrial fibrillation: implications for patient-specific antiarrhythmic drug therapy. *Eur Heart J* **38**:1764–1774.

Streit AK, Netter MF, Kempf F, Walecki M, Rinné S, Bollepalli MK, Preisig-Müller R, Renigunta V, Daut J, Baukrowitz T, et al. (2011) A specific two-pore domain potassium channel blocker defines the structure of the TASK-1 open pore. *J Biol Chem* **286**:13977–13984.

Wang L, Wible BA, Wan X, and Ficker E (2007) Cardiac glycosides as novel inhibitors of human ether-a-go-go-related gene channel trafficking. *J Pharmacol Exp Ther* **320**:525–534.

Wiedmann F, Schmidt C, Lugenbiel P, Staudacher I, Rahm AK, Seyler C, Schweizer PA, Katus HA, and Thomas D (2016) Therapeutic targeting of two-pore-domain potassium ($K_{(2P)}$) channels in the cardiovascular system. *Clin Sci (Lond)* **130**: 643–650.

Ziff OJ, Lane DA, Samra M, Griffith M, Kirchhof P, Lip GY, Steeds RP, Townend J, and Kotecha D (2015) Safety and efficacy of digoxin: systematic review and meta-analysis of observational and controlled trial data. *BMJ* **351**:h4451.

Address correspondence to: Dr. Dierk Thomas, Department of Cardiology, University of Heidelberg, Im Neuenheimer Feld 410, 69120 Heidelberg, Germany. E-mail: dthomas@ix.urz.uni-heidelberg.de